

ENHANCED SHIELDING AND MECHANICAL PROPERTIES OF WHITE CEMENT MORTARS VIA CELESTOBARITE FINE AGGREGATE

Yousra Hayouni¹, Wissem Gallala², Mohamed Essghaier Gaied³, Johann Plank⁴, Mohamed Bourham⁵ & Zeinab Alsmadi^{6}*

^{1,3}*Research Scholar, Laboratory of Mineral Resources and Environment, Department of Geology, Faculty of Sciences of Tunis, University of Tunis El Manar, 1060 Tunis, Tunisia*

¹*Research Scholar, Higher Institute of Water Sciences and Techniques, University of Gabes, 6072 Gabes, Tunisia*

²*Research Scholar, Research Unit of Geosystems, Georessources, Geoenvironments, Department of Earth Sciences, Faculty of Sciences of Gabes, University of Gabes, 6072 Gabes, Tunisia*

^{2,3}*Research Scholar, Higher Institute of Fine Arts, University of Sousse, Station Square, 4000 Sousse, Tunisia*

⁴*Research Scholar, Construction Chemistry, Technical University of Munich, Lichtenbergstraße 4, D-85748 Garching, Munich, Germany*

^{5,6*}*Research Scholar, North Carolina State University, Department of Nuclear Engineering, Raleigh, NC 27695-7909, USA*

ABSTRACT

This study emphasizes using barite mine wastes as aggregate material in blended mortar as an improved gamma-ray shielding structure in nuclear applications. Mortar mixtures made of white cement were prepared with various percentages of waste ranging from 0-30% as partial replacement of sand. Evaluation of density, flexural and compressive strength, and gamma-ray shielding were conducted. The increase in the percent of the barite wastes aggregates affects the gamma-ray attenuation coefficients. The results testified that the mine waste is appropriate as partial substitute to enhance gamma-ray shielding, ensures sustainability of natural resources and reduces the mortar and concrete costs.

KEYWORDS: *Celestobarite Mine Wastes, Fine Aggregate, Gamma-Ray Attenuation, Mortar, Mechanical Strength, Radiation Shielding*

Article History

Received: 16 Mar 2021 | Revised: 18 Mar 2021 | Accepted: 25 Mar 2021

INTRODUCTION

The increase in the use of natural resources as aggregates has contributed to increasing energy demand, pollution, toxicity of water, intensify climate change and depleting these materials causing critical shortages. The alarming rate at which materials are extracted has already a significant impact on the environment, human health and biodiversity. Thus, finding an alternative to compensate this irrational extraction of raw materials becomes an important subject. Recycling sector, which today accounts for one-tenth of the mining sector's weight of GDP (Gross Domestic Product), is expected to become more competitive and expand, but will continue to be much less massive than raw material extraction. Recent studies have shown the possibility of using various waste materials as alternatives of fine and coarse aggregates in mortar and concrete admixtures. This is to limit the increased use of natural aggregates and consequently save raw materials and environment

[1-8]. In North-east of Tunisia, the abandoned mine of “Hammam Jedidi” (since 1992) located in Zaghouan district [9] has generated a huge amounts of tailing materials, which counts about 2.35 Mt [10]. As described in literature [11, 12], these deposits correspond to a F-(Ba-Pb-Zn) mineralization associated with Jurassic lime stone; some heavy minerals such barite, Celestine, sphalerite, fluorite and galena might be found as residues in the wastes’ dumps [10, 13]. After ceasing mining activity, the huge dump of wastes poses harmful impacts on ecosystem by leaching heavy minerals into soil and groundwater. From there, it comes the idea of their recycling in order to contribute to ecosystem balance on the one hand and save raw materials on the other hand. Since celestobarite mine wastes admit physical specifications similar to natural sand (color, particle size, density, etc.), they might be used as partial replacement of fine and coarse aggregates in mortar and concrete admixtures specially knowing that they had not been extensively mentioned as fine aggregates in previous studies, in Tunisia at least. The use of barite as shielding material in the concrete goes back to the early 1950s [14, 15]. Furthermore, the presence of heavy minerals (lead, iron, magnetite, etc.) in these materials can make them effective in shielding ionizing radiation when incorporated into mortar mixture [1, 16-25]. Previous conducted researches [19, 20, 26-28] have mentioned that incorporation of heavy minerals as heavy aggregates in mortar and concrete confection seems effective and useful in gamma radiation attenuation even with minimal amounts. Moreover, several studies have demonstrated that the use of barite as aggregate and sand substitute, with an optimum content, has notably increased the linear attenuation coefficient [1, 16, 29-32]. Other studies have shown that the inclusion of barium oxide in barium borate glasses results in enhanced shielding properties against gamma-rays and fast neutrons [33], and that the increase in barium oxide increases the mass attenuation coefficient and reduces the half-value layer (HVL). Water to cement ratio (w/c) and compressive strength did not have any expressive effects on gamma-ray linear attenuation coefficient while material density has a relevant influence [17, 22, 32, 34]. Furthermore, the study performed by Akkurt, et al. [16] showed that the linear attenuation coefficient (μ) increases with the increasing materials’ density contrary to the mass attenuation coefficients (μ/ρ), which is kept constant. The experimental results displayed in most of the previous studies showed that the change in barite rate affects concrete’s physical and mechanical properties; some results showed that compressive and tensile strength decrease with the increase in barite content [35, 36]. However, results found by researchers reveal that increasing barite rate improves and enhances the mechanical properties of mortar [1, 34, 37].

The present study sheds light on the effect of incorporating Tunisian celestobarite wastes of Hammam Jedidi abandoned mine (North-Eastern Tunisia) on the attenuation of gamma-rays and the mechanical strength of mortar blended with the same mine waste. A comparison between the experimental results for normal concrete and that of barite tailing mortars was conducted. The relation between photon attenuation coefficients and materials bulk density was elucidated to evaluate the radiation shielding.

MATERIALS

Cement and Aggregate

The materials used in this study are:

- Ordinary Portland Cement CEM I 52.5 Nas classified by standard EN 197-1 and NT 47.01-1, supplied from SOTACIB cement plant for white cement, Feriana-Kasserine, Tunisia (Central west of Tunisia) [38, 39]. Its chemical composition is shown in Table 1. Table 2 shows the mineral content of Hammam Djedidi waste samples.

- Standard sand CEN, EN 196-1 provided from SNL (Société Nouvelle du Littoral) packaged in plastic bags dosed of $1350 \pm 5\text{g}$ with a specific grain size in accordance with EN 933-2 [40, 41].
- Fresh water.

Table 1(a): Average Chemical Composition of Cement and Hammam Djedidi Waste

	LOI	Na ₂ O	MgO	Al ₂ O ₃	SiO ₂	P ₂ O ₅	SO ₃	K ₂ O
CEM1 A/L	3.18	-	0.2	3.59	22.42	-	2.18	0.5
Waste	7.13	1.09	0.08	0.40	16.36	0.22	24.82	0.07

Table 1(b): Average Chemical Composition of Cement and Hammam Djedidi Waste

	CaO	TiO ₂	MnO	Fe ₂ O ₃	BaO	SrO	ZnO	Pb	F	Cl
CEM1 A/L	67.71	0.06	-	0.21	-	-	-	-	-	0.08
Waste	13.60	-	0.07	1.02	21.76	9.64	1.76	0.85	1.02	0.0004

Table 2: Mineral Content of Hammam Djedidi Waste Samples

Mineral	Amount %
Calcite	18.3
Barite	34.0
Quartz	21.1
Celestine	13.2
Fluorite	5.40
Sphalerite	2.10
Siderite	3.70
Amorphous phase	1.30

Celestobarite Mine Waste

Celestobarite mine wastes were sourced from the huge dump of Hammam Jedidi abandoned mine (Fig. 1(A, B)). The sampling was carried out by grooving the surface of the pack. Specimens were taken from the top, mid-height and the base of the dump (Fig. 1(C, D)). All samples were dried, mixed, weighed and quartering in order to obtain representative samples. A full analysis of a mean sample taken from three representative samples was carried out through a granulometric, mineralogical and chemical analysis. The grains distribution was performed using a laser particle sizer Analysette 22/NanoTec made by FRITSCHE GmbH (Germany). Chemical composition was carried out by X-ray fluorescence, the device used for X-ray spectroscopy is a PANalytical, B.V.Netherlands, Axios 2.4 KW using SUPER Q 4.0M software. For mineralogical characterization, measurements were performed on an X-ray powder diffract device: D8 Advance (Bruker AXS, Karlsruhe, Germany, Cu K α X-ray source, measurements recorded between 5 and 70° 2 θ) at room temperature. Evaluation of the different mineral compositions was calculated based on data obtained by XRD and Rietveld refinement, using Diffract plus EVA software V.8.0 and JCPDS PDF-2 database (JCPDS, 2003) for phase determination and Topas 4.0 (Bruker AXS, Karlsruhe, Germany) for quantitative XRD (Rietveld refinement). The content of main oxides of waste sample was determined by X-ray fluorescence with automated sample feed. The device used for X-ray spectroscopy is a PANalytical, B.V.Netherlands, Axios 2.4 KW using SUPER Q 4.0M software. This device, with automated sample feed, allows a non-destructive analysis of chemical composition in seconds expressed as oxides in wt.%. The beads were prepared by fusing mixtures of 1.65 g of powdered sample with 8.25 g of di-lithium tetraborate (Li₂B₄O₇) with 1:5 as sample to flux ratio. The main objective consists in the re-use and the management of these waste materials by incorporating them in mortar mixture as sand substitute in order to evaluate their effect on the attenuation of gamma-rays and the mechanical strength.

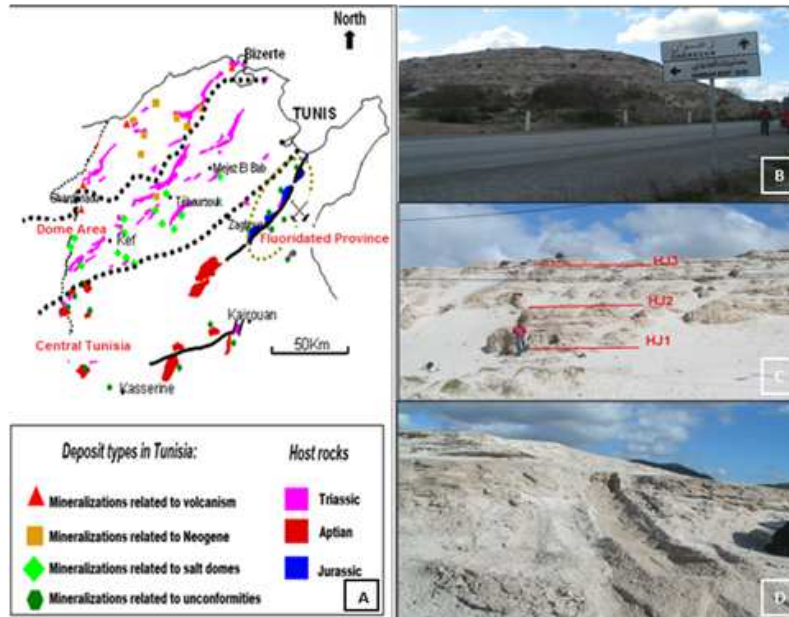


Figure 1. Hammam Djedidi Mine Waste Localization (ONM Modified) (A,B) and Channel Sampling (C,D).

METHODS

The procedure for mixing heavyweight concrete is similar to that for conventional concrete. Mortar mixtures made with natural standard sand (EN 196-1) were replaced by celestobarite mine waste (CBMW) in different proportions (5, 10, 15, 20, 25 and 30%) by weight of standard sand as shown in Table 3. Sample M3 was damaged and thus its results are irrelevant, however, kept in the record as few values may be considered.

Table 3: Mixture Proportion and Densities of Confectioned Mortars

Mixes	Density (g/cm ³)	Substitution ratio	Mortar Ingredients						Remarks
			Cement (g)	Water (g)	Standard Sand		Waste		
					%	g	%	g	
M ₁	2.32	0% (Blank/Reference)	450	225	100	1350	0	0	Bare: No Substitution
M ₂	2.20	5%	450	225	95	1282.5	5	67.5	
M ₃	2.67	10%	450	225	90	1215	10	135	Sample Damaged
M ₄	2.26	15%	450	225	85	1147.5	15	202.5	
M ₅	2.36	20%	450	225	80	1080	20	270	
M ₆	2.37	25%	450	225	75	1012.5	25	337.5	
M ₇	2.38	30%	450	225	70	945	30	405	

Mortar samples were prepared according to the Cement test method EN 196 1. Prismatic specimens 40x40x160 mm in size were processed to measure compressive strength at the curing ages of 2 and 28 days. Specimens molding was carried out with water to cement (w/c) ratio of 1:2 and kept constant for all specimens. After molding, specimens were stored in humid climate for 24 hours then stored immersed under water after de-molding until strength testing. The test was carried out using a 2000 kN compression testing machine and a loading rate of 0.6 MPa/s. A set of three prismatic specimens confectioned in a three-gang mold representing the curing time were used to set the compressive and flexural strength for each waste ratio. The measured density of mortars displayed in Table 3 was performed using a pycnometer. Gamma attenuation experiments were carried out through a standard 5 μCi radiation sources; one Ba-133 (0.356 MeV), one Cs-137 (0.662 MeV), and three Co-60 (1.173 and 1.333 MeV), and they were piled to each other to form an assembled

multi-photon energy source. Three Co-60 sources were stacked to produce a clearer and more defined spectrum of the 1.173 and 1.333 MeV photon peaks. The experimental setup, as described in Gallalla, et al. [1], used a 2"x2" sodium iodide (NaI) detector with built-in photomultiplier tube (PMT) with high voltage and electronics. Sources were placed 60 cm from the detector, and the total source height was 1.6 cm. The mortar sample was placed on a mesh holder away from the detector to eliminate buildup. Fig. 2 illustrates the source placement and the experimental setup for gamma attenuation measurements [1]. The experimental set up has collimators and the picture in the figure is with collimators removed to show the interior details. The source was collimated inside a lead cylinder. The detector was placed at a distance that avoids buildup. All measurements were taken with background corrected. Background is first measured and all measurements have the backgrounds subtracted. Linear and mass attenuation coefficients and half-value layer (HVL) were determined for the tested samples [1, 42]. MicroShield[®] version 9.05 package was used to calculate these values and compare them to experimental data [43].

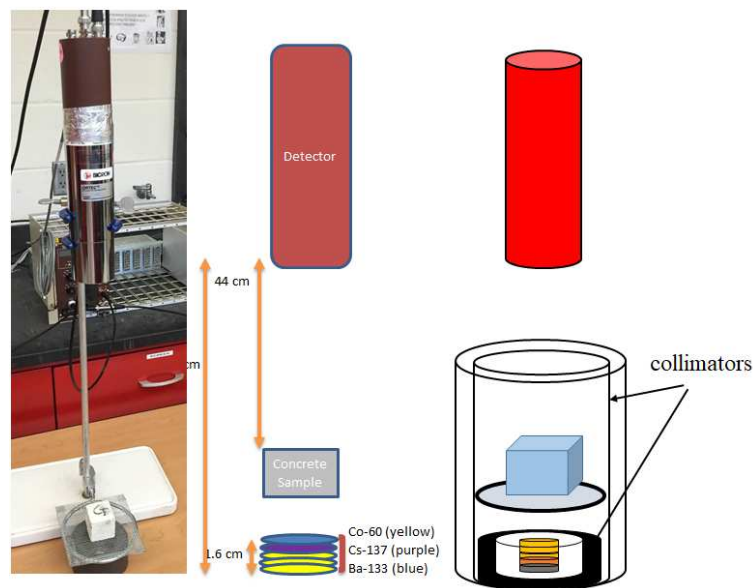


Figure 2: Experimental Setup for Gamma-Ray Attenuation Measurement (Picture taken with Collimation Removed).

RESULTS AND DISCUSSIONS

Waste Characterization

The mineral characterization of celestobarite waste sample using Rietveld refinement shows that barite (34%), quartz (22%), calcite (18%) and celestine (13%) are the main constituents of Hammam Djedidi waste materials (Table 3). The XRD diffractogram in Fig. 3 shows that the high intensities correspond to calcite; quartz and barium-strontian sulfate reflections and the low intensities correspond to galena and fluorite reflections.

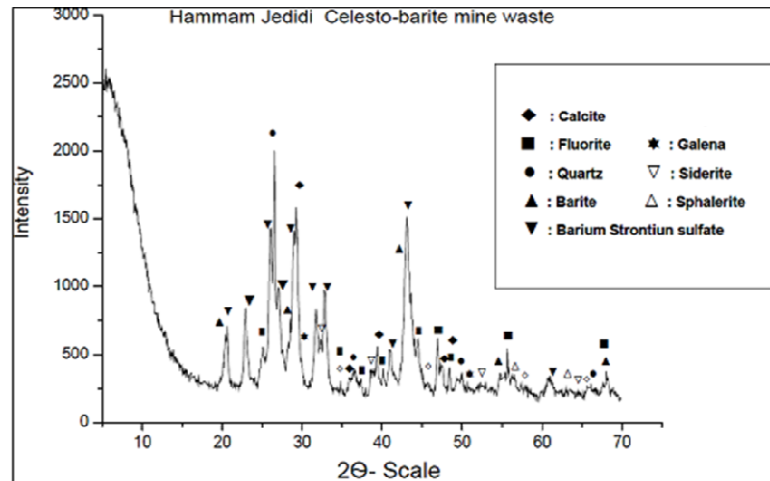


Figure 3: XRD Pattern of Hammam Djedidi Mine Waste.

These results are matching with the chemical composition given in Table 1, showing a high concentration of barium and silicon oxide reaching 21% and 16%, respectively, with a strontium oxide concentration of about 10%; and the composition given through the observation of polished thin section by polarized optical microscopy (POM) showing barite, fluorite, galena and quartz crystals (Fig. 4). The presence of heavy metals in relative high concentrations such as Pb (0.85%) and Zn (1.76%) make these waste materials hazardous and harmful to both human and environment.

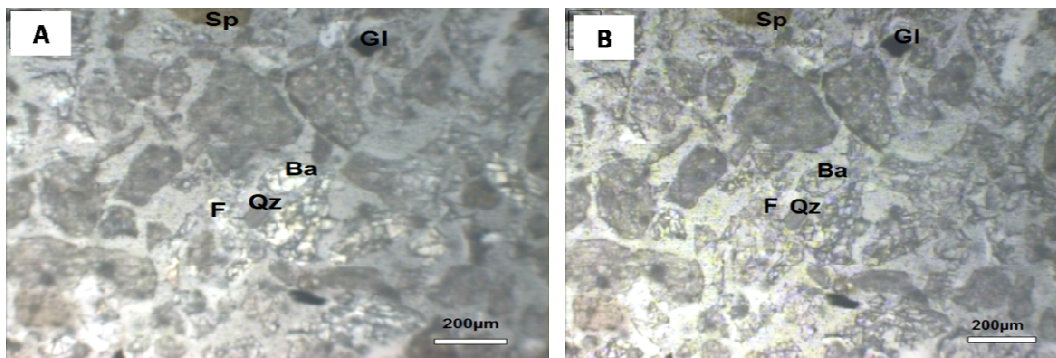


Figure 4: Optical Images of Waste Sample Under Plane Polarized Light (a) and Cross Polarized Light (b) (Ba: barite, F: fluorite, Gl: galena, Qz: quartz) [1].

Physical test data revealed a density of about 3.27 g/cm^3 ; thus, celestobarite mine waste could be classified as heavy weight aggregates as mentioned by Akkurt, et al. [18]. Consequently, concrete using these wastes as aggregates is called heavy or intermediate concrete. Concretes having specific gravities higher than 2600 kg/m^3 are called heavy-weight concrete and aggregates with specific gravities higher than 3000 kg/m^3 are called heavy-weight aggregates. Thus, the concrete where barite used as an aggregate in the concrete is one of the most approximately heavy or intermediate concrete. Granulometric analysis of waste sample plotted in Fig. 5 shows that the majority of particles have a size between $800 \mu\text{m}$ and $1 \mu\text{m}$. This indicates it is a fine material highly ranked with dominance of fine particles ($\Phi < 1 \text{ mm}$) referring to the most commonly used graphic measure, the median, based on taking the diameter that has half the grains (by weight) finer, and half coarser which is found by the intercept of the 50 percentile ($\Phi 50$) with the cumulative curve [44].

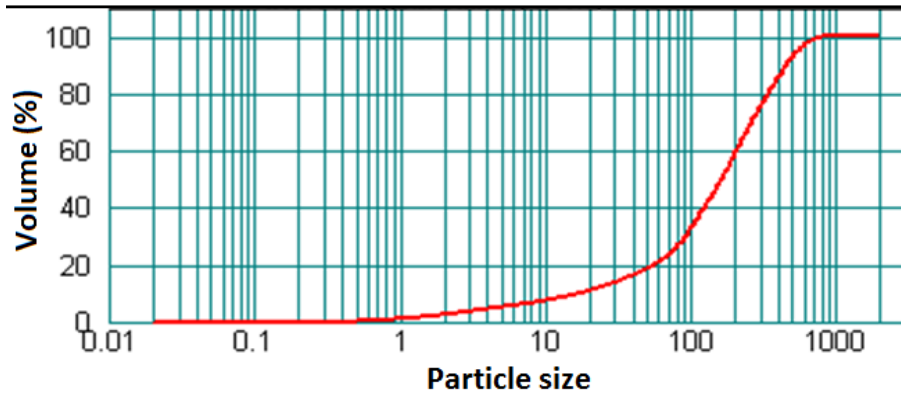


Figure 5: Particle Size of Hammam Djedidi Waste Sample.

Density

The measured density of hardened mortars is shown in Table 3 along with mixture proportions of each confectioned mortar specimen. As shown in the table, it is evident that specimens’ densities are approximately similar with a slight variation from a sample to another. This might be explained by the fact that sand substitution was based on total mass and not grain size distribution since the used cement (CEMI 52.5 N) has a specific gravity about 3.03 g/cm³ (Sotacib internal reports). Only the sample CBMW_10 ($\rho=2.67$) could be considered as heavy-weight mortar according to EN TS206-1 and UNE-EN [45], which classifies concrete greater than 2.6 g/cm³ as heavy-weight concrete.

Compressive Strength

Fig. 6 shows the compressive strength obtained for 28 days and is displayed as a function of waste rate in the hardened mortar. It is clear that the compressive strength has significantly increased with the increasing celestobarite ratio, reaching 59.8 MPa corresponding to 25% compared to 55.8 MPa for only 5% of sand substitution and compared to the reference sample. A slight decrease is noticed when the substitution exceeds 25%. The same behavior is observed at 2 days test. This might be related to the significant increase in the free water remaining than required in the mix for cement hydration [46]. The presence of free water with high waste ratio in the mixes affects particles arrangement inducing the creation of pores in the hardened mortar, which automatically leads to strength drop. Furthermore, compressive strength decline can be justified by the powerless association of barite minerals, due to angular shape of the grains, compared to the standard sand.

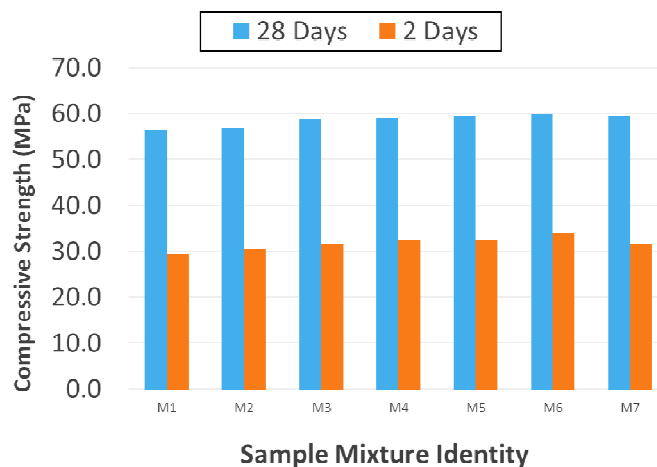


Figure 6: Compressive Strength of Hardened Mortars with Increasing Waste Ratios.

Flexural Strength

The bending flexural strength consists in carrying out flexural efforts in three or four points to generate the bending flexural test within the specimen, as specified in the NF EN 12390-5 standard [47]. For that, a prismatic test-tube of d_1, d_2 section and “L” range is used. The specimen to be placed within the apparatus so that the flatter faces are in contact with the rollers. The loading speed must be constant and between: $\sigma = 0.04$ and 0.06 MPa/s. The flexural strength is obtained as following in the case of a 3-point bending:

$$\sigma = \frac{3}{2} \left(\frac{FL}{d_1 d_2^2} \right) \tag{1}$$

Where F is the applied load in N and L, d_1 and d_2 in mm and σ in MPa. Results of the flexural test at 2 and 28 days are displayed in Fig. 7. As shown, the flexural strength values increase with increased substitution ratio and a slight decrease is observed when the replacement ratio exceeds 25%. These results are matching with those of compressive strength (same behavior) indicating a close relationship between the two parameters.

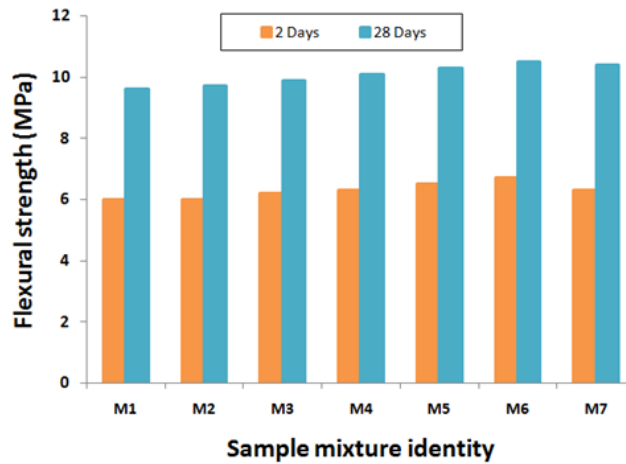


Figure 7: Flexural Strength of Hardened Mortars with Increasing Waste Ratios.

Leaching Test

Leaching test was examined for potentially toxic heavy metals: Hg, Cr, Zn, Cd, Pb and Cu using ICP Spectroscopy. The results are presented in Table 4 in which the measured values fall below the limits of the standards. These heavy metals are highly retained in the cement phases due to the alkaline pH, which inhibit leaching [3] and calcination and hydration [48]. As a result, the celestobarite mine waste can be used as secondary raw material reducing the exploitation of conventional natural resources.

Table 4: Results of Leaching Test (mg/Kg)

	Cd	Cr	Cu	Hg	Pb	Zn
Mortar	-0.077	0.678	0.336	0.017	0.106	0.128
Inert Waste (2003/33/EC)	0.04	4	2	0.05	0.5	4
Non-Hazardous Waste (2003/33/EC)	1	50	50	0.2	10	50

Attenuation Coefficients, HVL and MFP

The linear (μ) and mass (μ/ρ) attenuation coefficients of the studied mortar specimens were measured at photon energies of 0.356 (Ba-133), 0.662 (Cs-137), 1.173 and 1.333 (Co-60) MeV using the setup previously illustrated in Fig. 2. Results reveal that the linear and mass attenuation coefficients of SOTACIB’s mortar samples tend to decrease with increasing photon energy. The attenuation decreases significantly from 0.356 MeV to 0.662 MeV photon energy then slows for higher photon energies. This might be attributed to the dominance of photoelectric absorption and Compton scattering for low and intermediate energy gammas [32, 49, 50]. The results revealed that samples remaining 15-30% contents of celestobarite waste have approximately similar attenuation efficiency, as drawn in Fig. 8. The attenuation coefficients differ at different photon energies; samples with waste ratios greater than 10% are of high attenuations. This is due to the change in the specific density of the samples. It is also to be mentioned that while the composition of the sample, like sample M7, was as close to the actual composition as possible, there was some reformation in the samples after curing and this affects the sample homogeneity. The composition was incorporated in MicroShield[®], however, there is a deviation at low energies but the trend is reasonable. Samples M1 and M2 are of higher attenuations for 0.356 and 0.662 MeV energies than all other mixtures. Of importance is that samples with high attenuations have also high compressive strengths (59.8 MPa and 59.6 MPa, respectively), which sheds light on the relation between unit weight, compressive strength and radiation attenuation.

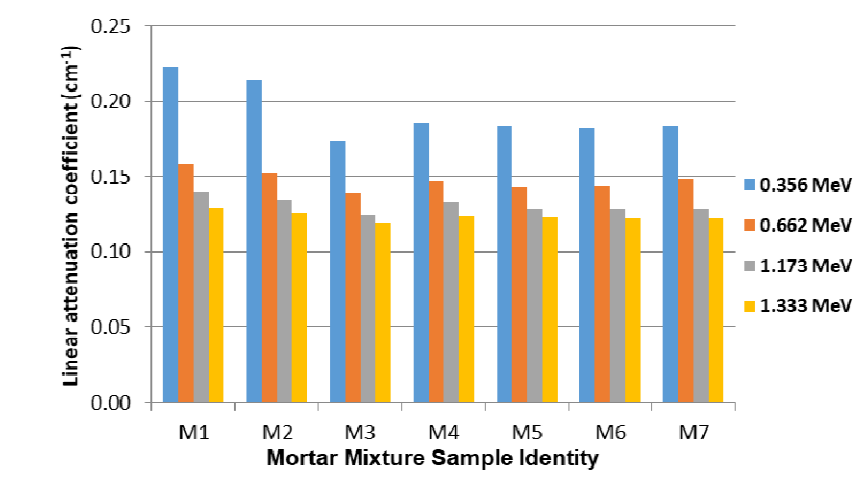


Figure 8: Linear Attenuation Coefficients of Waste Mortar Samples (M1: Reference Sample).

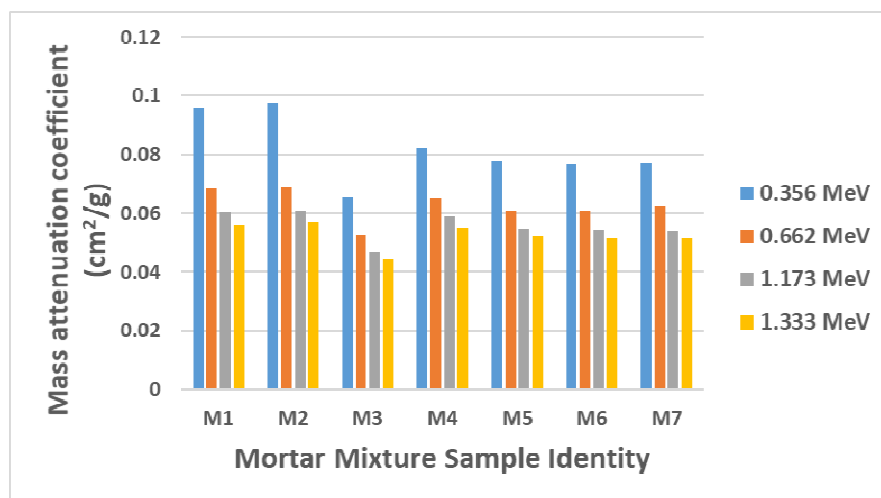


Figure 9: Mass Attenuation Coefficients of Waste Mortar Samples (M1: Reference Sample).

Linear attenuation coefficients were also computed using MicroShield® v9.05 based on the composition of each sample. A comparison between calculated and experimental values for mortar specimen M7 (30% of sand substitution) is shown in Fig. 10. It is clear that computed values generally lie within the experimental values with the exception for 0.356 Mev and 0.662 MeV photon energies. Computed linear attenuation coefficients indicated higher values when compared with the measured values. This difference is generally due to low homogeneity of samples or slight compositional differences. Compared to others types of mortar made with shielding materials, the studied mortar with 30% of barite waste is an effective material for using it in radiation shielding and has a linear attenuation coefficient very close to mortar (50% barite and 50% boron waste) at higher photon energies as illustrated in Fig. 11.

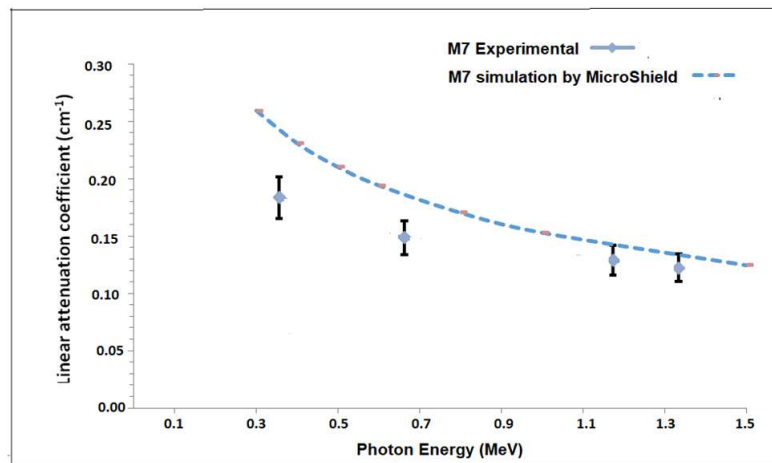


Figure 10: Measured and Calculated Gamma-Ray Linear Attenuation Coefficient of a Mortar Sample (Sample M7:30% of Waste Substitution) as a Function of Photon Energy.

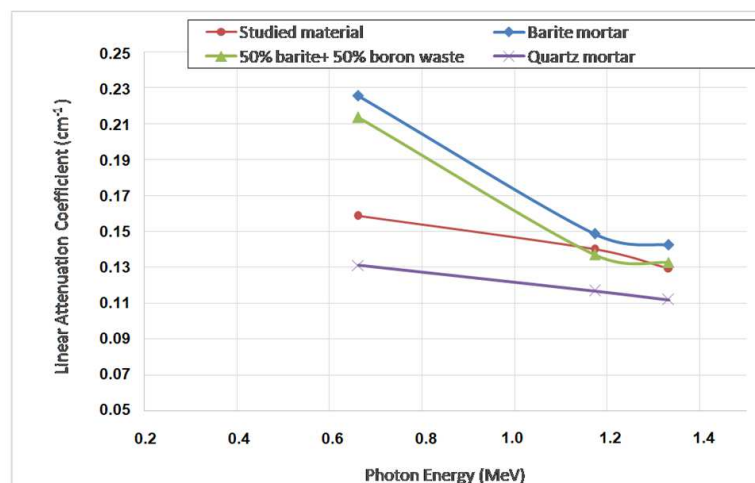


Figure 11: Comparison of Linear Attenuation Coefficients of Studied Materials and Ordinary, Barite, Serpentine and Boron Waste Mortars [1, 51].

The half-value layer (HVL) is determined from the thickness of the material that reduces the radiation intensity by half of the initial value as per the equation $HVL = \ln(2)/\mu$ [30, 52, 53]. Fig. 12 shows the variation of the half-value thickness of mortar samples, where the HVL increases with increasing photon energy. Furthermore, exposure rates with and without buildup were calculated for the photon energy range between 0.015 – 1.5 MeV showed that at the 0.015 MeV photon energy, the exposure rates are 6.4E-35 mR/hr with no buildup and 5.59E-35 mR/hr with buildup. However, the exposure rates differ at higher photon energy of 1.5 MeV with 2.03E-2 without buildup to 2.36E-2 with buildup.

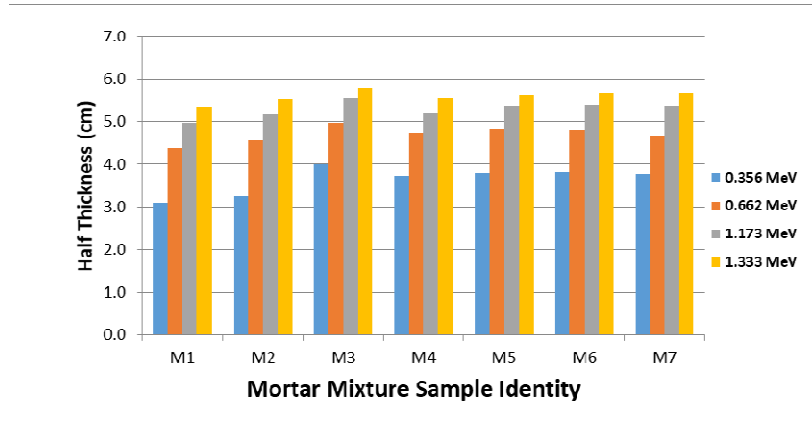


Figure 12: Variation of the Half-Value Thickness of Mortar Samples.

Figure 13 shows the variation of mean free path (MFP) of mortar samples at photon energies of 0.356 (Ba-133), 0.662 (Cs-137), 1.173 and 1.333 (Co-60) MeV. MFP is the average distance in which gamma radiation travels in the material before interacting. It is expressed as the reciprocal of the attenuation coefficient, $1/\mu$ [54, 55]. As shown in Fig. 12, MFP tends to increase with increasing photon energy, in which sample M7 (2.38 g/cm^3) exhibits the highest MFP at all photon energies while sample M1 (2.32 g/cm^3) exhibits the lowest MFP values at all energies.

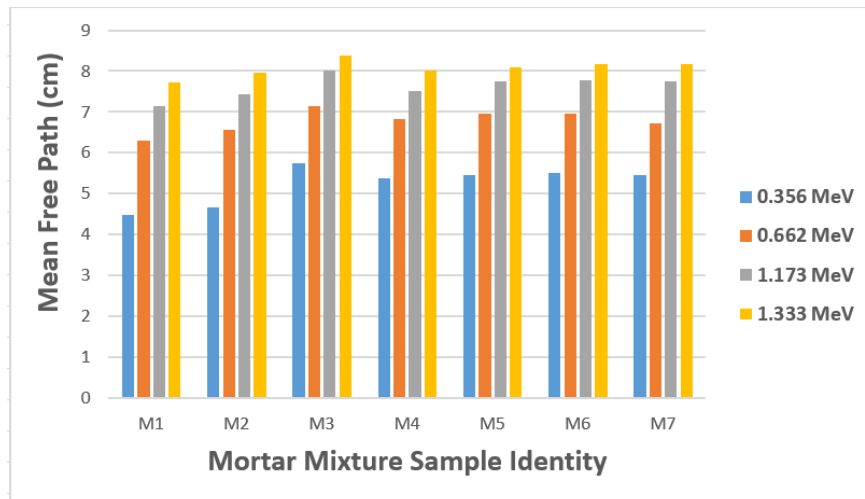


Figure 13: Variation of the Mean Free Path of Mortar Samples.

CONCLUSIONS

Protection against gamma radiation using celestobarite waste materials as heavy aggregates was experimentally investigated and compared to calculations of MicroShield[®]v9.05. For this purpose, heavy weight concrete samples containing waste barite aggregates were produced by partial replacement of standard sand. The participation percentages of heavy aggregates were selected as 0, 5, 10, 15, 20, 25 and 30%, respectively. The results revealed that samples remaining 15-30% contents of celestobarite waste have approximately similar attenuation efficiency. Theoretical attenuation coefficient values seem to be slightly higher than the experimental ones. Increasing heavy aggregates percentage up to 30% results in increasing the compressive strength (reached 59.8 MPa). Concrete with 25% barite waste provides better compressive and flexural strength and proves to be more economical than other concrete samples. Limiting the substitution of natural aggregates by barite waste was beneficial to both compressive strength and shielding ability, but in this case, barite mass ratio cannot exceed 20–30% (25% was the perfect substitution rate).

ACKNOWLEDGEMENTS

The authors acknowledge the research funding from University of Gabes, Tunisia and Department of Nuclear Engineering at North Carolina State University, USA. The present study is a part of one of the authors PhD thesis (Yousra Hayouni). The authors gratefully acknowledge Pr. Dr. Johann Plank (TUM Munich, Chair of Construction Chemistry) and his entire group of PhD students for accepting the PhD student to carry her internship under his supervision. The authors would like to thank technicians' staff from SOTACIB cement plant for white cement, Feriana Tunisia where concrete specimens were confectioned and cured. The authors would like to thank the technical personnel at North Carolina State University for their help during the course of this study. The authors express their sincere thanks to Ms. Jasmin Alsaied and Ms. Kathryn Bailey for their help in the radiation shielding experiments. Sincere thanks to Dr. Michael Fusco for his valuable comments and suggestions.

REFERENCES

1. Gallala, W., Hayouni, Y., Gaied, M. E., Fusco, M., Alsaied, J., Bailey, K. and Bourham, M. 2017. *Mechanical and radiation shielding properties of mortars with additive fine aggregate mine waste*. *Annals of Nuclear Energy*. 101, 600-606. <https://doi.org/10.1016/j.anucene.2016.11.022>.
2. Aksoğan O, Binici H, Ortlek E. 2016. *Durability of concrete made by partial replacement of fine aggregate by colemanite and barite and cement by ashes of corn stalk, wheat straw and sunflower stalk ashes*. *Constr. Build. Mat*. 106, 253-263, <https://doi.org/10.1016/j.conbuildmat.2015.12.102>.
3. Argane, R., Benzaazoua, M., Hakkou, R., Bouamrane, A., 2016. *A comparative study on the practical use of low sulfide base-metal tailings as aggregates for rendering and masonry mortars*. *J. CleanerProd*. 112, 914–925, <https://doi.org/10.1016/j.jclepro.2015.06.004>.
4. Kundu, S., Aggarwal, A., Mazumdar, S., Dutt, K.B., 2016. *Stabilization characteristics of copper mine tailings through its utilization as a partial substitute for cement in concrete: preliminary investigations*. *Environ. Earth Sci*. 75, 1–9. <https://doi.org/10.1007/s12665-015-5089-9>.
5. Shettima, A.U., Hussin, M.W., Ahmad, Y., Mirza, J., 2016. *Evaluation of iron ore tailings as replacement for fine aggregate in concrete*. *Constr. Build. Mater*. 120, 72–79. <https://doi.org/10.1016/j.conbuildmat.2016.05.095>.
6. Vignesh, S., Reddy, B.R., Nachiar, S.S., 2015. *Effect of partial replacement of natural sand with gold mine tailings on some properties of masonry mortars*. *International Journal of Engineering Research and Technology*, 4, 583-586.
7. Oritola, S., Saleh, A.L., Mohd Sam, A.R., 2014. *Performance of Iron Ore tailings as partial replacement for sand in concrete*. *Appl. Mech. Mater*. 735, 122–127. <https://doi.org/10.4028/www.scientific.net/AMM.735.122>.
8. Ugama, T.I., Ejeh, S.P., 2014. *Iron ore tailing as fine aggregate in mortar used for masonry*. *Int. J. Adv. Eng. Technol*. 7, 1170-1178.
9. Bouhleb, S, 1985. *Composition chimique, fréquence et distribution des minéraux de la série barytine-célestite dans les gisements de fluorine de Hammam Jédidi et Hammam Zriba-Jébel Guébli (Tunisie nord-orientale)*. *Bull. Minéral*. 108, 403-420, DOI:10.3406/bulmi.1985.7838.

10. Hayouni, Y., 2014. Valorisation des déchets miniers de fluoro-barytine de hammam jedidi dans l'amélioration des performances du ciment blanc. *Mémoire de mastère, Faculté des Sciences de Gabès*, p. 132.
11. Bouhleb, S., 1982. *Distribution du baryum et du strontium dans les gisements de la province fluorétunisienne; application aux gîtes de Hammam Jedidi et Hammam Zriba-Jebel Guebli Unpublished Ph. D. Thesis. Paul Sabatier university, Toulouse, France.*
12. Souissi, F., Souissi, R., Dandurand, J.L., 2010. The Mississippi Valley-type fluorite ore at Jebel Stah (Zaghouan district, north-eastern Tunisia): contribution of REE and Sr isotope geochemistries to the genetic model. *Ore Geol. Rev.* 37, 15–30. DOI:10.1016/j.oregeorev.2009.11.001.
13. Mhamdi, S., 2010. *Etude minéralurgique des rejets miniers de hammam jedidi. Mémoire de master, Faculté des Sciences de Tunis*, p. 126.
14. Gallaher, R. B., Kitzes, A. S. (1953). *Summary report on Portland cement concretes for shielding (No. ORNL-1414). Oak Ridge National Lab.*
15. Tirpak, E. G. (1954). *Report on design and placement techniques of barytes concrete for reactor biological shields. Engineering and Mechanical Division-Oakridge National Laboratory.*
16. Akkurt, I., Kilincarslan, S., Basyigit, C., 2004. The photon attenuation coefficients of barite, marble and limra. *Annals of Nuclear Energy.* 31, 577-582, <https://doi.org/10.1016/j.anucene.2003.07.002>.
17. Akkurt I, Basyigit C, Kilincarslan S, Mavi B, Akkurt A. 2006. Radiation shielding of concretes containing different aggregates. *CemConc Compos.* 28, 153-7.
18. Akkurt I, Altindag R, Basyigit C, Kilincarslan S., 2008. The effect of barite rate on the physical and mechanical properties of concretes under F–T cycle, *Mater. Des.* 29 1793–1795, <http://dx.doi.org/10.1016/j.matdes.2008.03.013>.
19. Fusco, M.A., Winfrey, L., Bourham, M.A., 2016. Shielding properties of protective thin film coatings and blended concrete compositions for high level waste storage packages. *Ann. Nucl. Energy* 89, 63–69. <https://doi.org/10.1016/j.anucene.2015.11.026>.
20. Waly, E., Bourham, M., 2015. Comparative study of different concrete composition as gamma-ray shielding materials. *Annals of Nuclear Energy.* 85, 306-310. <https://doi.org/10.1016/j.anucene.2015.05.011>.
21. Orlov, V.K., Metelkin, Y.A., Maslov, A.A., 2015. Extra-heavy concrete and cement: protective materials with enhanced c-ray absorption. *At. Energ.* 117, 243–250. DOI 10.1007/s10512-015-9917-5.
22. Binici, H., 2010. Durability of heavy weight concrete containing barite. *Int. J. Mater. Res.* 101, 1052–1059, DOI:10.3139/146.110360.
23. Binici, H., Aksogan, O., Sevinc, A.H., Kucukonder, A., 2014. Mechanical and radioactivity shielding performances of mortars made with colemanite, barite, ground basaltic pumice and ground blast furnace slag. *Constr. Build. Mater.* 50, 177–183, <http://dx.doi.org/10.1016/j.conbuildmat.2015.05.020>.
24. Kilincarslan, S., Akkurt, I, Basyigit, C. 2006. The effect of barite rate on some physical and mechanical properties of concrete, *Mater. Sci. Eng. A.* 424, 83–86. <https://doi.org/10.1016/j.msea.2006.02.033>.

25. Gaikwad, D. K., Sayyed, M. I., Botewad, S. N., Obaid, S. S., Khattari, Z. Y., Gawai, U. P., Pawar, P. P., 2019. Physical, structural, optical investigation and shielding features of tungsten bismuth tellurite-based glasses. *Journal of Non-Crystalline Solids*, 503, 158-168. <https://doi.org/10.1016/j.jnoncrysol.2018.09.038>.
26. Makarious, A.S., Bashter, I.I., Abdo, A.E.S., Azim, M.S.A., Kansouh, W.A., 1996. On the utilization of heavy concrete for radiation shielding. *Ann. Nucl. Energy*. 23, 195–206. [https://doi.org/10.1016/0306-4549\(95\)00021-1](https://doi.org/10.1016/0306-4549(95)00021-1).
27. Obaid, S. S., Sayyed, M. I., Gaikwad, D. K., Tekin, H. O., Elmahroug, Y., & Pawar, P. P., 2018 a. Photon attenuation coefficients of different rock samples using MCNPX, Geant4 simulation codes and experimental results: a comparison study. *Radiation Effects and Defects in Solids*, 173(11-12), 900-914. <https://doi.org/10.1080/10420150.2018.1505890>.
28. Obaid, S. S., Gaikwad, D. K. and Pawar, P. P., 2018b. Determination of gamma ray shielding parameters of rocks and concrete. *Radiation Physics and Chemistry*. 144, 356-360. <https://doi.org/10.1016/j.radphyschem.2017.09.022>.
29. Shams, T., Eftekhar, M., Shirani, A., 2018. Investigation of gamma radiation attenuation in heavy concrete shields containing hematite and barite aggregates in multi-layered and mixed forms. *Construction and Building Materials*. 182, 35-42. <https://doi.org/10.1016/j.conbuildmat.2018.06.032>.
30. Ali Delnavaz; Aniseh Salavatiha; Amir Kalhor. 2017. Effective parameters in gamma radiation transmission rate from heavy concrete with iron oxide and barite aggregates. *Journal of materials in civil engineering* 29(9),04017140, [https://doi.org/10.1061/\(ASCE\)MT.1943-5533.0001979](https://doi.org/10.1061/(ASCE)MT.1943-5533.0001979).
31. Süleyman Gökçe H, Yalçinkaya C., Tuyan M., 2018. Optimization of reactive powder concrete by means of barite aggregate for both neutrons and gamma rays. *Construction and Building Materials* 189 (2018) 470–477. <https://doi.org/10.1016/j.conbuildmat.2018.09.022>.
32. Akkurt, I., Basyigit, C., Kilincarslan, S., Mavi, B., 2005. The shielding of γ -rays by concretes produced with barite. *Progress in Nuclear Energy*. 46, 1-11, <https://doi.org/10.1016/j.pnucene.2004.09.015>.
33. Al-Buriah, M. S., Sriwunkum, C., Arslan, H., Tonguc, B. T., Bourham, M. A., 2020. Investigation of barium borate glasses for radiation shielding applications. *Applied Physics A-Materials Science & Processing*. 126(1), 68, <https://doi.org/10.1007/s00339-019-3254-9>.
34. Ouda, A.S., 2014. Development of high-performance heavy density concrete using different aggregates for gamma-ray shielding. *Housing and Building National Research Center (HBRC), Dokki, Giza, Egypt*. 11, 328-338. <https://doi.org/10.1016/j.pnucene.2014.11.009>.
35. Esen, Y., Yilmazer, B., 2010. Investigation of some physical and mechanical properties of concrete produced with barite aggregate. *Scientific Research and Essays*. 5, 3826-3833.
36. Saidani, K., Ajam, L., Ouezdou, M.B., 2015. Barite powder as sand substitution in concrete: Effect on some mechanical properties. *Constr. Build. Mater.* 95, 287-295. DOI: 10.1016/j.conbuildmat.2016.05.095.
37. Yildizel Sadik Alper, 2017. Effects of Barite Sand Addition on Glass Fiber Reinforced Concrete Mechanical Behavior. *Int J Eng Appl Sci*. 9, 100-105. <http://dx.doi.org/10.24107/ijeas.366441>.

38. European Committee for Standardization (CEN). (2012). EN 197-1. Cement—Part 1. Composition, specifications and conformity criteria for common cements.
39. NT 47.01-1. Cement-Part1: Composition, specifications and conformity criteria for common cements.
40. CEN, EN 196-1, 2005. Methods of testing cement, Part 1. Determination of Strength.
41. EN 933-2., 1997. Tests for geometrical properties of aggregates. Determination of particle size distribution. Test sieves, nominal size of apertures.
42. Akkurt, I., Canakci, H., 2011. Radiation attenuation of boron doped clay for 662, 1173 and 1332 keV gamma rays. *Iran J. Radiat. Res.* 9, 37-40.
43. MicroShield, Grove Software, <http://radiationsoftware.com/microshield/>.
44. Trask, P. D. 1930. Mechanical analysis of sediment by centrifuge. *Economic Geology* 25, 581-599.
45. EN TS206-1.,2002. Concrete-Part-1: Specification, Performance, Production and conformity. Turkish Standards Institution, Ankara.
46. Al-Jabri, K.S., Al-Saidy, A.H., Taha, R., 2011. Effect of copper slag as a fine aggregate on the properties of cement mortars and concrete. *Constr. Build. Mater.* 25, 933–938. <https://doi.org/10.1016/j.conbuildmat.2010.06.090>.
47. NF EN 12390-5 Testing hardened concrete part 5 flexural strength of test specimens.
48. Zhang, J., Liu, J., Li, C., Nie, Y., & Jin, Y. (2008). Comparison of the fixation of heavy metals in raw material, clinker and mortar using a BCR sequential extraction procedure and NEN7341 test. *Cement and concrete research*, 38(5), 675-680.
49. Erdem, M., Baykara, O., Dog̃ru, M., Kuluöztürk, F., 2010. A novel shielding material prepared from solid waste containing lead for gamma ray. *Radiat. Phys. Chem.* 79, 917–922, <https://doi.org/10.1016/j.radphyschem.2010.04.009>.
50. El-Khayatt, 2010. Radiation shielding of concretes containing different lime/silica ratios. *Ann. Nucl. Energy* 37, 991–995. <https://doi.org/10.1016/j.anucene.2010.03.001>.
51. Çelen, Y. Y., Evcin, A., Akkurt, I., Bezir, N. Ç., Günoğ̃lu, K., & Kutu, N. 2019. Evaluation of boron waste and barite against radiation. *International Journal of Environmental Science and Technology*, 16, 5267-5274. <https://doi.org/10.1007/s13762-019-02333-3>.
52. Mann, H.S., Brar, G.S., Mann, K.S., Mudahar, G.S., 2016. Experimental Investigation of clay fly ash bricks for gamma-ray shielding. *Nucl. Eng. Technol.* 48, 1230–1236. <https://doi.org/10.1016/j.net.2016.04.001>.
53. Tarim, U.A., Ozmutlu, E.N., Gurler, O., Yalcin, S., Gundog̃du, O., Sharaf, J.M., Bradley, D.A., 2013. Monte Carlo modelling of single and multiple Compton scattering profiles in a concrete material. *Radiat. Phys. Chem.* 85, 12–17. <https://doi.org/10.1016/j.radphyschem.2012.10.018>.

54. Zeinab Y. Alsmadi, Mohamed Bourham. *Shielding Properties of Alloy 709 Advanced Austenitic Stainless Steel as Candidate Canister Material in Spent Fuel Dry Casks. International Journal of Physics and Research, vol. 10, Issue. 2, pp. 11-26 (2020).*
55. Zeinab Y. Alsmadi, Mohamed A. Bourham. *Shielding Properties of 316 Stainless Steel with Multi-layered barriers for Spent Fuel Drycasks. International Journal of Physics and Research, vol. 11, Issue. 1, pp. 5-20 (2021).*